Structural and electronic structural properties of ordered LiAl compounds

X.-Q. Guo, R. Podloucky,* and A. J. Freeman
Department of Physics and Astronomy, Northwestern University, Evanston, Illinois 60208
(Received 12 January 1989)

Precise results of first-principles electronic-structure calculations of the structural and electronic properties of the binary compound LiAl are presented for the bcc-based $B32$ and $B2$ crystal structures, the fcc-based $L1_0$ and the simple-cubic-based $B1$ structures as obtained with the full-potential linearized augmented-plane-wave method. Particular care was taken to ensure the convergence of the total energy as a function of the inherent numerical parameters in order to obtain as precise absolute total energies as possible. Our results corroborate the findings of recent previous studies about the electronic bonding in LiAl, as well as the existence of a high-pressure phase transition from $B32$ to $B2$ that we find at 140 kbar. Band structures, densities of states, total energies, and charge densities are presented and discussed. Good agreement with experimental data concerning the equilibrium properties is found.

I. INTRODUCTION

The binary LiAl compound is of some theoretical as well as technological interest because of its peculiar bonding properties[1] and because of its application as an electrode material for high-energy-density batteries. Several studies have been reported[2–4] on the electronic structure of LiAl concerning the nature of the bonding and also the structural competition between two bcc-like phases.[3,4] The present paper presents results of an electronic-structure calculation based on the full-potential linearized augmented-plane-wave[5] (FLAPW) method which makes no shape approximation to the potential nor needs any restrictions concerning the basis functions. Furthermore, the total energy as a function of all inherent parameters (such as the number of plane waves and the cutoff of the l expansion as well as the number of $\mathbf{k}$ points for the Brillouin-zone integration) was converged to high precision. Therefore, our results may be considered as the most precise local-density calculation for the LiAl compound available at present. In addition, they also serve as a key part of an extensive study on the Al-Li alloy system[6,7] by means of first-principles calculations of the electronic structure of ordered compounds.

For these investigations, the basic ingredient is the total electronic energy as a function of volume for a large number of ordered structures. It needs to be emphasized that high precision is needed for the study of the Al-Li alloy system because of the structural competition between the stable $B32$ and a metastable Al_3Li compound of $L1_2$ structure which is of interest for technological applications.[8] Finally, for a detailed understanding of the electronic bonding (and also in the framework of our investigation of the whole Al-Li alloy system) we also took into account fcc-based $L1_0$ ("Cu-Au–I") and simple-cubic-based $B1$ ("NaCl") structures in addition to the stable $B32$ ("Zintl") crystal structure and to the $B2$ ("CsCl") structure.

II. COMPUTATIONAL APPROACH

The first-principles full-potential linearized augmented-plane-wave method was applied to calculate the self-consistent electronic structures and total energies of LiAl binary compounds having the $B32$, $B2$, $L1_0$, and $B1$ crystal structures (Fig. 1). Special attention was paid to the precision of the results by studying the convergence of the total energy as a function of all necessary parameters. The l expansion for the wave function, charge density, and potential was truncated at $l=10$. About 50 basis functions per atom were used to build up the Hamiltonian and about 1000 plane waves for the representation of the charge density and potential in the interstitial region. The number of basis functions was increased up to 100 per atom and the plane wave for charge density and potential was increased to 2000 for testing. The difference in total energy was found to be less than 0.01 mRy. Muffin-tin radii were chosen to be equal for both atomic species (2.44 a.u. for $B32$ and $B2$ and 2.50 a.u. for $L1_0$ and $B1$ crystal structures). The linear tetrahedron method was employed to perform Brillouin-zone integrations. Particular care was taken to converge the total energy as a function of the number of $\mathbf{k}$ points according to Ref. 5. In general, 250–300 $\mathbf{k}$ points in an irreducible wedge of the first Brillouin zone were taken into account in the final runs resulting in an error in the absolute total energies smaller than 0.1 mRy. For the exchange-correlation part of the local-density approximation the approach of Hedin and Lunqvist[9] was employed.

III. RESULTS

A. Total energy and ground-state properties

Table I summarizes the results of our calculation of total energies. The volume-dependent quantities were obtained by a parabolic fit of the total-energy–

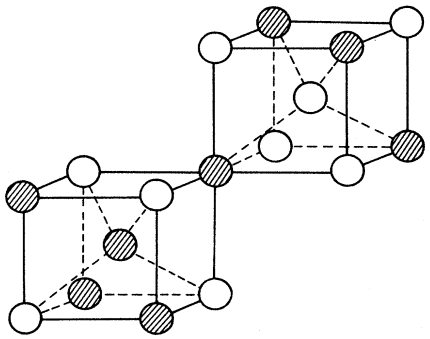

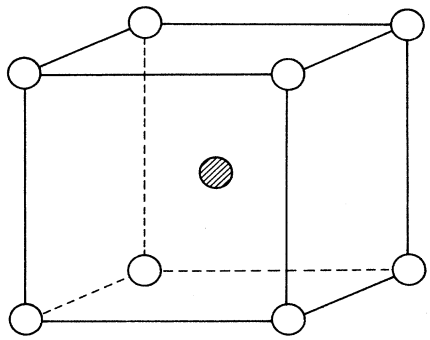

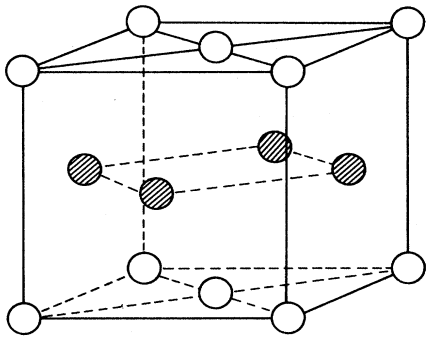

FIG. 1. Cubic unit cells of $B32$ ("Zintl"), $B2$ ("CsCl"), and $L1_0$ ("Cu-Au–I") crystal structures.

versus–volume results. As mentioned above, all the parameters inherent in the calculation were expanded until sufficient convergence of the total energy was reached. Special attention was paid to the dependence of the total energy on the number of **k** points for the Brillouin-zone integration. This dependence can be different for different cases, for different compositions as well as for compounds with different crystal structures but with the same composition. For example, within the linear tetrahedron method for Al about 3000 **k** points in the irreducible wedge would be necessary for a convergence of the absolute value of the total energy to within 1 mRy. This estimate was obtained by extrapolation[5] of the results for many total-energy–versus–**k**-point-number results up to 1000 **k** points. In contrast to Al, in the case of Li only 200 **k** points are sufficient for a precision smaller than 0.1 mRy. For the LiAl compounds, we found that about 300 **k** points in the irreducible wedges of the different structures are required for the final convergence of 0.1 mRy.

Figure 2 shows the total energy versus volume for the $B32$, $B2$, and $L1_0$ structures. The crossing of the stable $B32$- and the $B2$-structure total-energy curves corroborates the prediction of a structural phase transition found by Christensen[3] and Hafner and Weber.[4] Overall, our results agree with those of Christensen's lineal muffin-tin-orbital (LMTO) calculation. We predict a phase transition at 140 kbar for a lattice-parameter decrease of $\sim 5\%$ compared with 200 kBar and $\sim 4\%$ in the LMTO case. This similarity is due to the similar $B32$-$B2$ separation energies of -13.2 mRy (FLAPW) and -11.6 mRy (LMTO). But the bulk moduli are substantially different because our result (0.58 Mbar) is 30% larger than the LMTO result (0.45 Mbar). For this reason, we predict the phase transition at lower pressures although the $B32$ structure is more stable in our case. There is also good agreement between the two calculations for the equilibrium lattice parameter (11.821 and 11.960 a.u. for FLAPW and LMTO, correspondingly) but both are smaller than experiment (12.020 a.u.).[10] For the energy of formation we obtain -44.8 kJ mol^{-1} (where per mol is per AlLi pair), which is in reasonable agreement (within 10%) with the experimental result[10] of -48.6 kJ mol^{-1}. The result of the LMTO calculations of Christensen[3] (-49.8 kJ mol^{-1}) turns out to be closer to the experimental value than the FLAPW results which, from a theoretical point of view, are considered to come from a

TABLE I. Total energy (in Ry) per formula unit, lattice parameter a (in a.u.), atomic radius R (in a.u.), bulk modulus (in Mbar), and energy of formation ΔH_f and cohesion ΔH_c (in Ry).

Structure	E	a	R	B	ΔH_f	ΔH_c
$B32$	−498.7108	11.821	2.910	0.58	−0.0336	−0.499
$B2$	−498.6976	5.841	2.876	0.42	−0.0204	−0.486
$L1_0$	−498.6972	7.465	2.917	0.50	−0.0200	−0.486
$B1$	−498.6560	9.934	3.081	0.28	0.0212	−0.444
Al+Li (fcc)	−498.6772	7.769	3.036	0.48		−0.465
Al (fcc)	−483.8420	7.538	2.946	0.82		−0.295
Li (fcc)	−14.8352	8.000	3.126	0.14		−0.170
Al (atom)	−483.547					
Li (atom)	−14.665					

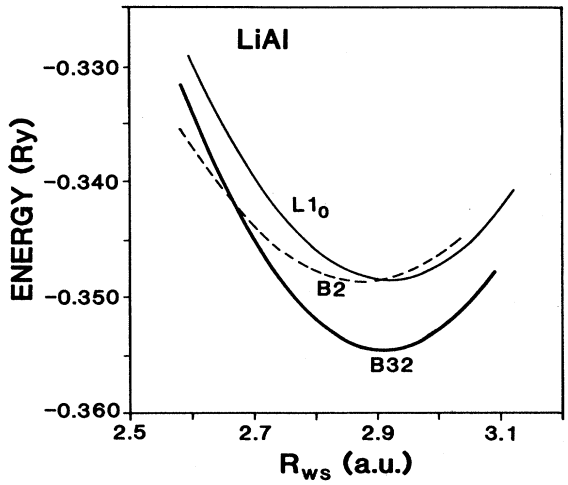

FIG. 2. Total energy per atom for LiAl vs atomic radius for the $B32$, $B2$, and $L1_0$ structures.

more precise method. One should be cautious, however, in making comparisons because of the wide scattering of the experimental data and the fact that LiAl is known for its formation of vacancies and antisite atoms even for the stoichiometric composition.

Larger differences are found when comparing our results to the recent study of LiAl by Hafner and Weber[4] based on a first-principles linear-combination-of-atomic-orbitals (LCAO) method. They get a substantially smaller energy difference (2.4 mRy) for the $B32$-$B2$ structures and therefore they predict a phase transition at much lower pressures. Furthermore, their equilibrium lattice parameter (12.056 a.u.) is larger by $\sim 2\%$ compared to our result, and even larger than (although very close to) the experimental value. For the volume of formation (change of volume at compound formation) they obtain -8.8% in comparison to our value of -11.9% and to the experimental result of -14.9%. In general, both our study and the study of Christensen seem to describe somewhat stronger bonding effects than does the LCAO calculation.

In our study we also included the fcc-based $L1_0$ and the simple-cubic-type $B1$ structures. The $B1$ rocksalt structure is of simple-cubic type when all the lattice points are occupied by the same type of atoms. These are artificial structures for LiAl in the sense that they cannot be made experimentally. For the $B1$ case this is quite obvious from Table I because it even has a positive formation energy. As discussed later on for the charge density, the local environment is unfavorable for bonding because of the negative pressure of rather free-electron-like states. In a simple picture one might think about Li atoms (nearest neighbors to Al) squeezing their valence electrons in between the fcc Al-Al sublattice (second-nearest neighbors). The situation is quite different for the $L1_0$ structure. Its total energy is nearly the same as for the $B2$ structure (only 0.4 mRy higher), but it cannot be stabilized because of its too large bulk modulus. Again, as discussed later for the charge density, this behavior can be understood by the formation of planarlike bonds of Al atoms in pure Al planes.

The structural competition discussed above is beautifully illustrated by the structure map of Pettifor.[11] In this map one locates LiAl in the $B32$ field quite close to some $B2$-structure compounds. $L1_0$ or even $B1$-structure compounds are well separated from the $B32$-structure domain. It is interesting to note that LiAl is very close to a domain of the "CrB" structure which is of orthorhombic type, quite close to the compound GaBa. Therefore, one might speculate that an orthorhombic distortion might drive $B32$-structure LiAl to a structural phase transition.

B. Charge density

To illustrate the nature of the bonding we show in Fig. 3 contour plots of charge densities for the $B32$, $B2$, and $L1_0$ structures. The [110] cut through Al and Li atoms of Fig. 3(a) shows the interesting feature of pronounced Al—Al bonds connecting the nearest-neighbor Al atoms of the Al diamond-type sublattice. Apart from minor details, Christensen,[3] by applying the "pseudo-muffin-tin-orbital" approach, obtained very similar results for the [110] charge distribution. In our case, the Al—Al bond charge is slightly more localized in the Al-Al direction as revealed by the magnitude and the shape of the contours. We obtain a maximum somewhere between 3.5 and 4.0 in units of 10^{-2} [number of electrons/(a.u.)^3] whereas Christensen's value lies in the range of 3.0 to 3.25. Based on a self-consistent LCAO method, Hafner and Weber[4] also seem to get a slightly higher pileup of charge density for the Al—Al bond but the spacings of their contours is too large for a more precise statement.

In discussing the nature of the bonding in $B32$-structure LiAl, Refs. 3 and 4 refer to a mixture of covalent bonding, as expressed by the Al-Al diamond-type bonds, and metallic bonding, as indicated by the rather uniform electron distribution in the Li-Li direction. Figure 3(b) illustrates the metallic type of bonding by showing a large region of rather uniform charge distribution. (In this figure the charge density is cut by a [111] plane through Li atoms.) The other contours originate from Al atoms in the centers of the cubes with length $a/2$ (see Fig. 1). Their charge distribution is distorted in the direction of the nearest-neighbor Al atoms at the corners of the cubes with one of them located perpendicular to the one in the figure. Also a [100] cut through planes of alternating Al and Li, which we do not show here, reveals metallic-bonding behavior.

For the case of the $B2$ structure, as can be seen from Fig. 3(c), the bonding is rather metalliclike without any strong Al—Al bonds. The reason is that the smallest Al-Al distance (5.841 a.u.) is much larger than for the $B32$ structure (5.119 a.u.) as can be calculated from the lattice parameters of Table I. (For comparison, the nearest-neighbor distance of pure fcc Al, a classic example of metallic bonding, is 5.330 a.u.) Furthermore, the atomic coordination is quite different in these two cases. Considering the environment of Al, for the $B2$ structure there

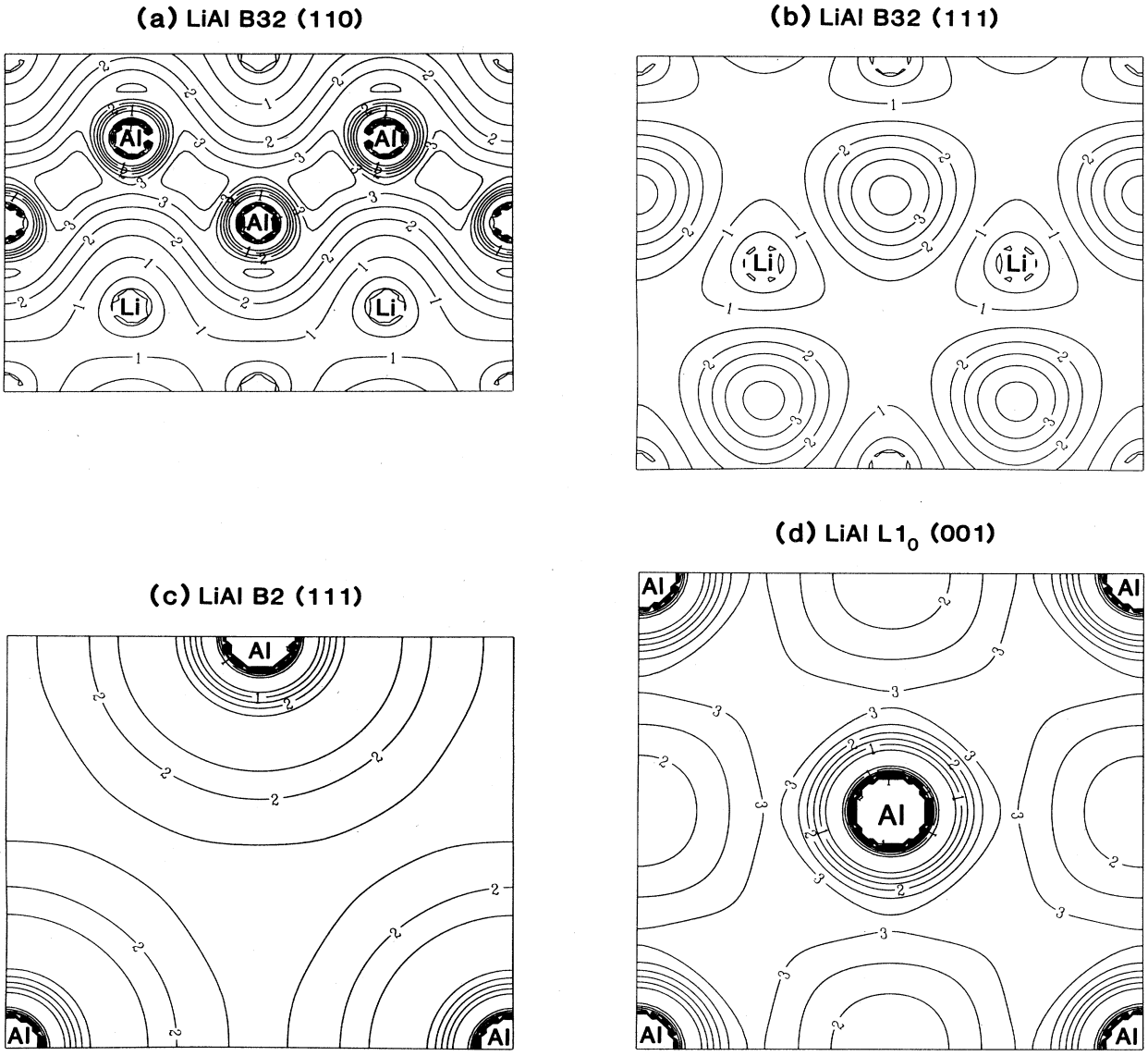

FIG. 3. Charge-density contour plots for the $B32$ [(a) and (b)], $B2$ (c), and $L1_0$ (d) structures in units of 10^{-2} [(number of electrons)/(a.u.)^3].

are eight nearest-neighbor Li atoms at cube centers and six Al atoms, but only as second-nearest neighbors at corner points; for the $B32$ case one finds the eight nearest-neighbor atoms, namely four Al and four Li, at the corner points of a cube of length $a/2$ (see Fig. 1). Interestingly, the atomic volumes at equilibrium are also quite different for these two structures—as can be seen from Fig. 2. The atomic volume of the $B2$ structure (Wigner-Seitz $R_{WS}=2.876$ a.u.) is smaller by 3.5% compared to the $B32$ case ($R_{WS}=2.910$ a.u.). [Again compare with pure fcc Al which has an atomic volume ($R_{WS}=2.946$) that is 3.7% larger than the $B32$ structure case.]

From these results, we can derive a simple picture for the bonding situation in the $B2$ structure geometry. The Al atoms of the $B2$ structure want to form stronger bonds by coming closer together, but the negative pressure of the electron gas as provided by the Li atoms counteracts this tendency. If sufficient external pressure is applied, the Al—Al bonding becomes strong enough to make the $B2$ structure the most stable one. The system is thereby driven to a $B32 \rightarrow B2$ structural phase transition as expressed by the crossing of the total-energy curves in Fig. 2. The distinctly different type of bonding is also expressed by the differences of the bulk moduli; the $B2$-structure modulus (0.42 mBar) is smaller by 25% than the $B32$-structure value (0.58 Mbar). In changing the volume of the $B32$ structure, one has to work against the pronounced Al—Al bonds [Fig. 3(a)] which costs more energy than changing the volume of the $B2$ case where metallic bonding is dominant.

As shown in Fig. 3(a), the four Al nearest neighbors

form strong bonds. From the point of view of the local environment there is another simple structure, the $L1_0$ structure, which has four Al nearest neighbors (Fig. 1). It is an fcc-based lattice with 12 nearest neighbors, four Al atoms, and eight Li atoms. The differences from the $B32$ structure consist of (i) the number and positions of nearest-neighbor Li atoms and (ii) the spatial arrangement of the nearest-neighbors Al atoms which are now located in planes. This planar arrangement is emphasized by the charge-density contours of Fig. 3(d) where a [001] plane cuts through Al atoms only [Fig. 1(c)]. As for the $B32$ structure we again find a pileup of charge in between the Al atoms. A cut, which is not shown here, perpendicular to the pure Al planes reveals rather flat contours in between the Al planes indicating a layerlike electron distribution. The Al-Al nearest-neighbor distance in the $L1_0$ structure (5.279 a.u.) is much closer to that in the $B32$ than in the $B2$ structure, and therefore Al atoms can form bonds similar to (but slightly weaker) than that of the $B32$ structure shown in Fig. 3(a). Also the atomic volume ($R_{WS}=2.917$ a.u.) is very close to that of the $B32$ structure case. The bulk modulus of 0.50 Mbar lies precisely in between the $B2$ and $B32$ structure values indicating the intermediate situation also for the bonding of pronounced but less strong Al—Al bonds and an appreciable amount of metallic bonding.

If we compare the total energies (Fig. 2) we find that, at equilibrium, the $L1_0$ structure is as stable as the $B2$ structure (a difference of only 0.4 mRy) but there is no chance of a structural phase transition because of (i) the larger bulk modulus and (ii) the larger atomic volume. The Al—Al bonds are not strong enough to allow for a $B32 \rightarrow L1_0$ structural phase transition, partially because the Al-Al distance for the $L1_0$ case is somewhat larger. But also the planar arrangement of Al atoms must be energetically less favorable for sp^3 hybrids compared with the geometrically different $B32$ structure bonds. From that, one might speculate that appropriate lattice distortions might result in a structural phase transition from a distorted $B32$ structure to a distorted $L1_0$ structure geometry. A quite common crystal structure of binary compounds is the simple-cubic-based $B1$ rocksalt structure. According to our results (Table I) this structure even has a positive formation energy. We might interpret this situation in terms of the pressure of electrons provided by the six nearest-neighbor Li atoms which drive the Al atoms of the metallic Al sublattice (the Al atoms occupy an fcc lattice as in pure Al) with an Al-Al nearest-neighbor distance of 7.024 a.u. On the other hand, the Al-Li distance of 4.967 a.u. is the smallest of all structures under discussion but close to the $B2$ structure case (5.058 a.u. as compared to 5.119 and 5.278 a.u. for the $B32$ and $L1_0$ structures, respectively). The $B1$-structure bulk modulus (0.28 Mbar) is much closer to pure Li (0.14 Mbar) than to any other LiAl compound (Table I).

C. Band structure

The band-structure results for the $B32$ crystal structure below and around the Fermi energy [cf, Fig. 4(a) and Table II] is rather similar to the case of a single diamond lattice.[12,13] For example, one finds sp-like bands along $\Gamma-X$ which merge into twofold-degenerate bands for the $X-W$ direction. The slope of the $\Gamma-X$ bands is not horizontal at point X. This and the occurrence of pronounced Al bonds, as shown by the charge-density contour plot of Fig. 3(a) suggest a simple model of bonding by taking into account only the nearest-neighbor Al atoms. In that case the Li atoms are considered to just donate electrons for the Al—Al bonds. Following these ideas, we applied a two-center tight-binding model according to Slater and Koster[12] by taking into account only s and p states, and we obtained the parameters of Table III. The fit was done by hand for states at points X, Γ, and L for which we can easily factorize the Hamiltonian. With these parameters we calculated the band structure of Fig. 4(b) which essentially looks very similar to the FLAPW result if we just consider the lowest bands. There are a few differences, such as the small but finite dispersion of the bands along $X-W$ where the tight-binding model yields straight bands. These bands reflect the second-nearest-neighbor interactions as can be concluded from the dispersive $X-W$ bands of diamond[13] (i.e., of a single diamond lattice type). Another much more important difference can be found at point X where for the FLAPW calculation a band is lowered below the Fermi energy. Because of this, the energy gap which occurs in the tight-binding band structure disappears, making LiAl a semimetal. At this point the Al-Li interaction becomes more important as can be derived from the decomposition of charges within the muffin-tin spheres. For this state at point X we find dominant Li s character which contains 12% of the total charge as compared with only 7% Al s. All other states below the Fermi energy are of dominant Al character, e.g., the L point just below E_F is of Al p character (23%) in comparison to 2% of Li p charge. But the next higher state at point L changes its character to 17% Li p and only 5% Al p type. At point Γ the changes from Al to dominant-Li character occur at higher energies.

For the $B2$ structure the situation is quite different because of the distinctly different local environment. The Al atoms are surrounded by eight Li nearest-neighbor

TABLE II. Energy eigenvalues in rydbergs (relative to the Fermi energy) of the $B32$ structure at points Γ, X, and L. (The degeneracy of the states is given in parentheses.)

Γ	−0.672 (1)	−0.023 (3)	0.055 (3)	0.210 (1)	0.306 (3)
X	−0.446 (2)	−0.326 (2)	−0.010 (2)	0.505 (2)	0.517 (2)
L	−0.553 (1)	−0.404 (1)	−0.059 (2)	0.028 (2)	0.063 (1)

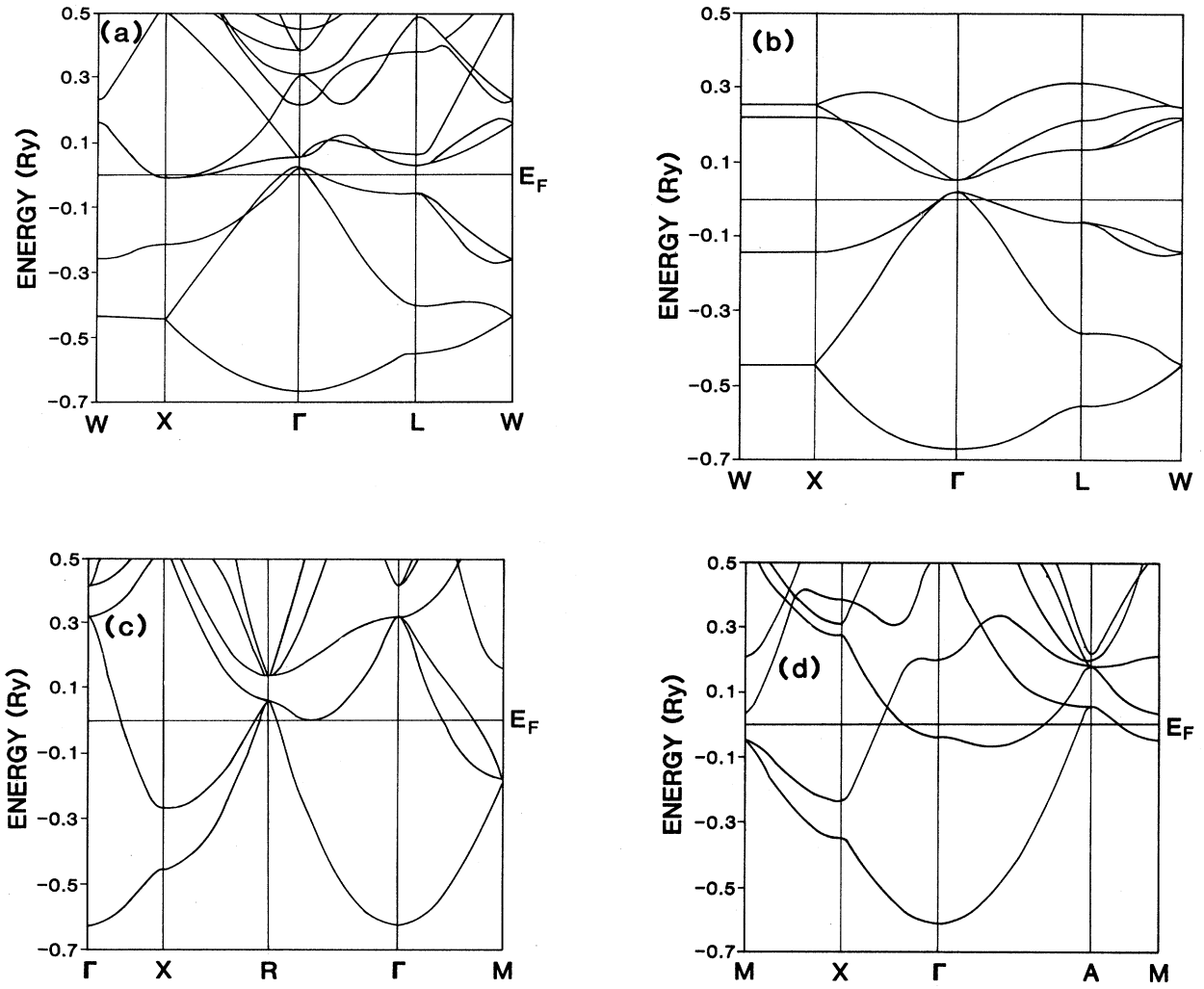

FIG. 4. Band structure of LiAl for the crystal structures (a) $B32$ and (b) $B32$ determined by a tight-binding approach (see Table I) plotted relative to the Fermi energy of $B32$ [shown in (a)], (c) $B2$, and (d) $L1_0$.

atoms in contrast to the $B32$ structure case where four Al and four Li atoms occupy the nearest-neighbor shell. Therefore the bands show large dispersions of a rather free-electron type which suggest that the Li atoms donate valence electrons into the space between the atoms as demonstrated by the charge density shown in Fig. 3(b).

To understand the band structure of the $L1_0$ crystal structure, we note that the local environment is again changed. Now, because it is an fcc-type lattice, the Al atoms have 12 nearest-neighbor atoms but only four of them are Al atoms. One might consider the $L1_0$ structure as pure planes of Al atoms separated by pure planes of Li atoms. Again, the Al atoms form bonds with their Al neighbors [Fig. 3(c)] but these are somewhat weaker than the tetrahedral bonds of the $B32$ structure. We again tried a simple tight-binding model by just rescaling the two-center parameters of Table III assuming a $1/r^3$ dependence for the pp matrix elements and a $1/r^2$ and a $1/r$ dependence for the sp and ss matrix elements, respectively. The changes due to rescaling are quite small. However, the resulting tight-binding band structure is less satisfactory compared to the FLAPW results than was the case for the $B32$ structure. Therefore, a simple model of the bonding in the $L1_0$ structure just in terms of Al bonds in planes is not quite adequate although the weak dispersion of the three lower FLAPW bands along $A-M$ [Fig. 4(d)] indicates pronounced in-plane interactions. The tight-binding model gives straight bands for this case because the $A-M$ direction vector is perpendicular to the Al planes. Further, in contrast to the results

TABLE III. Two-center tight-binding parameters (Ry) for the $B32$ structure with nearest-neighbor Al-Al interactions only. The atomic levels E_s^0, E_p^0 are given relative to the Fermi energy.

E_s^0	E_p^0	$(ss\sigma)$	$(sp\sigma)$	$(pp\sigma)$	$(pp\pi)$
−0.231	0.039	−0.110	0.140	0.094	−0.041

of the tight-binding model of Al planes, the nonnegligible interlayer and Al-Li interactions are demonstrated by the two different lowest bands which are not degenerate at point X.

D. Density of states

The density of states (DOS) of the $B32$ structure [Fig. 5(a)] shows pronounced features reflecting the peculiar bonding occurring in this material. There are three main peaks which can be identified from the band structure of Fig. 4(a). The lowest sp-bonding L state at -0.533 Ry gives rise to the lowest peak in the DOS which is separated by a gaplike minimum from the next-lowest peak. This minimum is seen to arise from the bands shown in Fig. 4(a) at this energy where the bands merge into twofold-degenerate states, which is generally true for all states of a diamond structure[12] at the X point. Although the DOS value at this minimum is very small, a gap cannot be formed because of the diamond symmetry.

The peak (at -0.36 Ry) above this minimum comes from sp antibonding states of the second-lowest $L-W$ band. Above the next (less pronounced) minimum (at -0.28 Ry), one finds the two Al p bonding peaks of the Al sublattice. The lowest of these peaks is due to states of an $L-W$ band close to point W. The second peak is split off because of the small but finite dispersion of the second lowest $X-W$ band. Above the third minimum just below E_F, the Al antibonding states are hybridized with Li states resulting in a multipeaked but less characteristic DOS. Because the Fermi energy falls into a strongly rising peak of the density of states, one expects an electronic instability which is probably related to the peculiar vacancy properties of $B32$-structure LiAl. The density of states of the $B2$ structure case [Fig. 5(b)] shows two peaks below the Fermi energy but resembles a rather free-electron-like case as can be seen in the charge density of Fig. 3(b).

For the $L1_0$ structure [Fig. 5(c)] we discussed a planar-like bonding behavior [see also the charge density of Fig. 5(c)] which is partially expressed by the two rectangular shaped structures of the DOS below the E_F which would characterize a two-dimensional electron gas.

As a convenient summary and for easy comparison, Table IV presents FLAPW results for the density of states at the Fermi energy and illustrates the quite different types of bonding for the three different structures.

IV. CONCLUDING REMARKS

On the basis of our precise first-principles approach, we studied the energetics and bonding properties of the binary compound LiAl and found for the stable $B32$-structure phase a mixture of covalent and metallic bonding—thereby corroborating recent studies.[3,4] The formation of diamondlike bonds (concerning the geometry but, of course, not the strength) of the nearest-neighbor Al-Al atoms stabilizes the $B32$ structure as

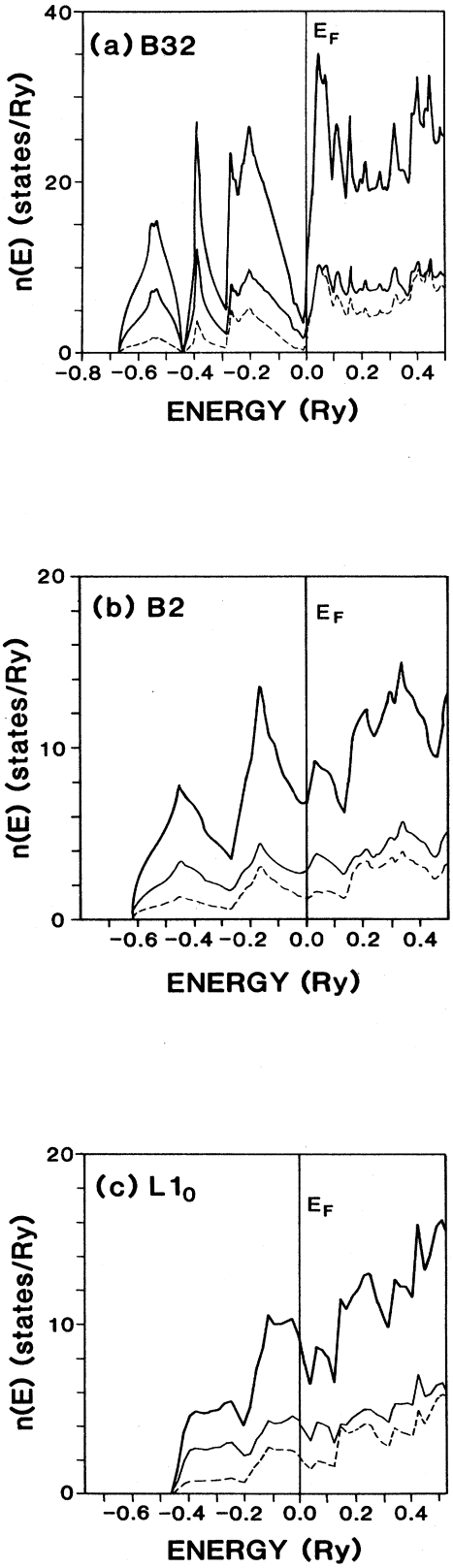

FIG. 5. Density of states $n(E)$ for LiAl (in units of states/Ry cell) for (a) $B32$, (b) $B1$, and (c) $L1_0$ structures. Thick solid line, total $n(E)$; thin solid line, Al partial $n(E)$; thin dashed line, Li partial $n(E)$.

TABLE IV. Density of states (in states/Ry cell) at the Fermi energy, $n(E_F)$, and the integrated density of states, N, normalized to 8.0 electrons per cell. $N(E_F)$ is decomposed into its contributions from the interstitial region (N_{int}) and the muffin-tin spheres.

			Al				Li			
Structure	n	n_{int}	n_s	n_p	n_d	n_{sph}	n_s	n_p	n_d	n_{sph}
$B32$	9.0	2.9	1.1	1.5	1.0	3.5	1.6	0.5	0.4	2.5
$B2$	13.0	5.4	1.6	3.3	0.5	5.4	0.3	1.4	0.5	2.2
$L1_0$	18.6	5.5	1.2	6.6	0.9	8.7	0.5	3.1	0.7	4.2
			Al				Li			
Structure	N	N_{int}	N_s	N_p	N_d	N_{sph}	N_s	N_p	N_d	N_{sph}
$B32$	8.0	2.6	1.7	2.1	0.2	4.0	0.5	0.9	0.1	1.5
$B2$	8.0	3.4	1.5	1.4	0.1	3.0	0.5	0.9	0.1	1.5
$L1_0$	8.0	2.4	1.8	1.9	0.2	3.9	0.6	1.0	0.1	1.7

compared with the $B2$-structure phase and allows a phase transition at 140 kbar. Although the total energy of the $L1_0$ structure is only 0.2 mRy higher than for the $B2$ structure case, no structural phase transition to a $L1_0$-structure phase is possible because of its higher bulk modulus, which is due to its formation of planar Al—Al bonds. The energetics and equilibrium properties appear to be in good agreement with experiment.

ACKNOWLEDGMENTS

This work was supported by the Air Force Office of Scientific Research (Grant No. 85-0358), U. S. Department of Defense, by a computing grant at the Wright-Patterson Air Force Base Supercomputing center and by the Austrian Ministry of Science (Project No. 49-55413-24187).

*Present address: Institute for Physical Chemistry, University of Vienna, Währingerstrasse 42, A-1090 Vienna, Austria.

[1]E. Zintl and P. Wolterdorf, Z. Elektrochem. **41**, 876 (1935); E. Zintl and G. Brauer, Z. Phys. Chem. B **20**, 245 (1933); W. Hückel, *Structural Chemistry of Inorganic Compounds* (Elsevier, Amsterdam, 1951).

[2]A. Zunger, Phys. Rev. B **17**, 2582 (1978); T. Asada, T. Jarlborg, and A. J. Freeman, *ibid.* **24**, 857 (1981).

[3]N. E. Christensen, Phys. Rev. B **32**, 207 (1985).

[4]J. Hafner and W. Weber, Phys. Rev. B **33**, 747 (1986).

[5]H. J. F. Jansen and A. J. Freeman, Phys. Rev. B **30**, 561 (1984).

[6]R. Podloucky, X.-Q. Guo, H. J. F. Jansen, and A. J. Freeman, Phys. Rev. B **7**, 5478 (1988).

[7]M. Sluiter, D. de Fontaine, X.-Q. Guo, R. Podloucky, and A. J. Freeman (unpublished).

[8]G. Cocco, S. Fagherazzi, and L. Schiffini, J. Appl. Crystallogr. **10**, 325 (1977); D. B. Williams and J. W. Edginton, Metall. Sci. **9**, 529 (1975).

[9]L. Hedin and S. Lundqvist, J. Phys. C **4**, 2064 (1971).

[10]I. Barin, O. Knacke, and O. Kubaschewski, *Thermochemical Properties of Inorganic Substances* (Springer, Berlin, 1977), Suppl.

[11]D. G. Pettifor, Solid State Commun. **51**, 31 (1984); and J. Phys. C **19**, 285 (1986).

[12]J. C. Slater and G. F. Koster, Phys. Rev. **94**, 1498 (1954).

[13]A. Zunger and A. J. Freeman, Phys. Rev. B **15**, 5049 (1977).